

# Reformulating non-equilibrium steady-states and generalised Hopfield discrimination

Uğur Çetiner<sup>1</sup>, and Jeremy Gunawardena<sup>1,†</sup>

<sup>1</sup>Department of Systems Biology, Harvard Medical School, Boston, MA 02111, USA

<sup>†</sup>Corresponding author: Jeremy Gunawardena (jeremy@hms.harvard.edu)

ABSTRACT

Markov processes are widely used to model stochastic systems in physics and biology. Their steady-state (s.s.) probabilities are given in terms of their transition rates by the Matrix-Tree theorem (MTT). The MTT uses spanning trees in a graph-theoretic representation of the system and reveals that, away from thermodynamic equilibrium, s.s. probabilities become globally dependent on all transition rates and the resulting expressions grow super-exponentially in the graph size. The overwhelming complexity and lack of thermodynamic insight have impeded analysis, despite substantial progress elsewhere in non-equilibrium physics. Assuming Arrhenius rates with vertex energies and edge barrier energies, we show that the s.s. probability of vertex  $i$  is proportional to the average of  $\exp(-S(P))$ , where  $S(P)$  is the entropy generated along a minimal path,  $P$ , from  $i$  to a reference vertex. The average is taken over a Boltzmann-like probability distribution on spanning trees, whose “energies” are their total edge barrier energies. This reformulation offers a thermodynamic interpretation that smoothly generalises equilibrium statistical mechanics and it reorganises the expression complexity: the number of distinct minimal-path entropies depends on the number of edges where energy is expended, not on graph size. We demonstrate the power of this reformulation by extending Hopfield’s analysis of discrimination by kinetic proofreading to any graph in which energy is expended at only one edge, for which we derive a general formula for the s.s. error ratio.

# INTRODUCTION

Equilibrium thermodynamics and statistical mechanics are among the great success of 19th century physics and remain essential for studies in many fields. In contrast, despite impressive advances, the foundations of non-equilibrium physics remain under development. This gap has had significant repercussions in biology, since life itself is quintessentially a far from equilibrium phenomenon. Although much is known about the molecular components involved in energy transduction, the functional significance of energy expenditure has been harder to unravel, especially for cellular information processing.

The biophysicist Terrell Hill introduced in the 1960s an approach to analysing individual non-equilibrium entities, such as a membrane transporter or a motor protein, based on mesoscopic states and transitions—essentially a Markov process—represented in “diagrammatic” form—essentially a graph [15, 16]. Jürgen Schnakenberg developed this approach further in the 1970s in his “network theory” [30]. An important contribution of these studies was to show how graph cycles related macroscopic thermodynamic quantities like entropy production to the underlying stochastic mesoscopic quantities. For reasons that remain unclear, this graph-based approach then disappeared from sight in the physics literature. In particular, it played no role in the renaissance of non-equilibrium statistical mechanics which began in the 1990s and has led to exact fluctuation theorems for systems arbitrarily far from thermodynamic equilibrium [10, 13, 19, 21, 22, 24, 7]. As physicists began to build on these new findings, Markov processes became a foundational tool for stochastic thermodynamics [31] and their graph-based representations began to be rediscovered [1, 23, 27].

Graphs also make an appearance in the pioneering work of Wentzell and Freidlin in large deviation theory [33, 12]. Here, the graph offers a discrete approximation to a stochastic differential equation in the limit of low noise or low temperature. Vertices correspond to stable steady states, edges to appropriate barrier crossings and labels to crossing rates. Such graph-theoretic approximations have been further developed within chemical physics, especially for analysing complex free-energy landscapes at thermodynamic equilibrium [34, 4].

Independently of these developments, a graph-theoretic approach to analysing biochemical systems under timescale separation, the “linear framework”, was introduced in systems biology

[14, 26, 25, 38, 39]. This was applied to bulk populations of biochemical entities, such as post-translational modification systems [8, 28], but the same mathematics can be used to analyse individual stochastic entities, such as genes [9, 3, 36, 29, 37]. In this context, as in the approaches described above, the linear framework provides a treatment of continuous-time, finite state Markov processes based on directed graphs with labelled edges. Vertices correspond to mesostates, directed edges to transitions and edge labels to transition rates. The main distinction with the approaches described above is that the graph is treated as a mathematical entity in its own right. This offers a rigorous way to relate network structure to function that is well-suited to rising above the molecular complexity found in biology [35, 36].

The graph-theoretic approach offers particular insight into a problem which has resisted the breakthroughs in non-equilibrium statistical mechanics mentioned above: the probabilities of mesoscopic states, even at steady-state, remain intractable to exact analysis. We explain the issues here in broad terms before giving full details below.

The s.s. probabilities of a Markov process can be expressed in terms of its graph edge labels by using certain subgraphs—spanning trees—as described by the Matrix-Tree theorem (MTT, Eq.3). Results of this kind date back to Kirchhoff [20]. The version used here was first stated by Tutte [32] but independently rediscovered by Hill [15] and by many others [26]. The MTT makes clear that, as soon as the system is away from thermodynamic equilibrium, even if that occurs through energy expenditure at only a single edge, the s.s. probabilities become globally dependent on all edge labels in the graph. The resulting expressions, which depend on enumerating all spanning trees, become extremely complex. Consider, for example, a graph whose mesostates correspond to the presence or absence at  $k$  sites of some feature, such as binding of a ligand, so that there are  $2^k$  mesostates. For  $k = 2$ , there are 4 spanning trees; for  $k = 3$  there are 384 spanning trees; but for  $k = 4$  there are 42,467,328 spanning trees [9]. All of these trees are required to exactly determine s.s. probabilities. Moreover, while the mathematical details are clear, a thermodynamic interpretation of these expressions has been lacking. We have not been able to see the wood for the trees. The combinatorial complexity and lack of thermodynamic meaning have greatly hindered exact calculations, even for systems which are, from an equilibrium perspective, very straightforward.

We offer a solution to both these challenges. Since the complexity cannot be avoided, it must be reorganised and reinterpreted. There are two parts to this reformulation. First, we define a

probability distribution on spanning trees rooted at a reference vertex, 1. To do this, we write the edge labels in Arrhenius form, in terms of a vertex energy and an edge barrier energy; our constructions are independent of the choices involved. Surprisingly, in view of the non-equilibrium setting, the distribution on trees is Boltzmann-like, with  $\Pr(T) \propto e^{-E(T)}$ , where the energy  $E(T)$  is the sum of the barrier energies on all edges of the tree  $T$  (Eq.8). We call this probability distribution the “arboreal distribution”. Second, we focus on minimal paths in the graph from a given vertex,  $i$  to 1. Minimal paths are those with no repeated vertices; there are only finitely many such and each spanning tree rooted at 1 yields a unique minimal path from  $i$  to 1. Let  $S(P)$  denote the overall entropy production from taking the path  $P$ . Detailed balance tells us that the equilibrium s.s. probability of vertex  $i$  is proportional to  $\exp(-S(P))$ , no matter what path  $P$  is chosen from  $i$  to 1. Our main result is that, away from thermodynamic equilibrium, the s.s. probability of vertex  $i$  is proportional to the average of  $\exp(-S(P))$ , where  $P$  runs over minimal paths from  $i$  to 1 and the average is taken over the arboreal distribution (Eq.10). The use of path averages in our reformulation has similarities with other types of results in non-equilibrium statistical mechanics, as we review in the Discussion.

Our reformulation not only provides a thermodynamic interpretation in place of a forest of trees, it also finesses the combinatorial explosion. This is because the number of distinct values for the entropy production on minimal paths has a different scaling to the number of spanning trees or the number of minimal paths themselves. The scaling does not depend on the size of the graph; rather it depends on how many edges in the graph are experiencing energy expenditure (below). This revised scaling dramatically simplifies the calculation of s.s. probabilities.

To illustrate the power of this reformulation we substantially generalise Hopfield’s classic study of discrimination by kinetic proofreading [17]. Hopfield analysed a simple graph with 3 vertices. We analyse any graph in which energy is expended at only one edge and give a general formula for the error ratio (Eq.18).

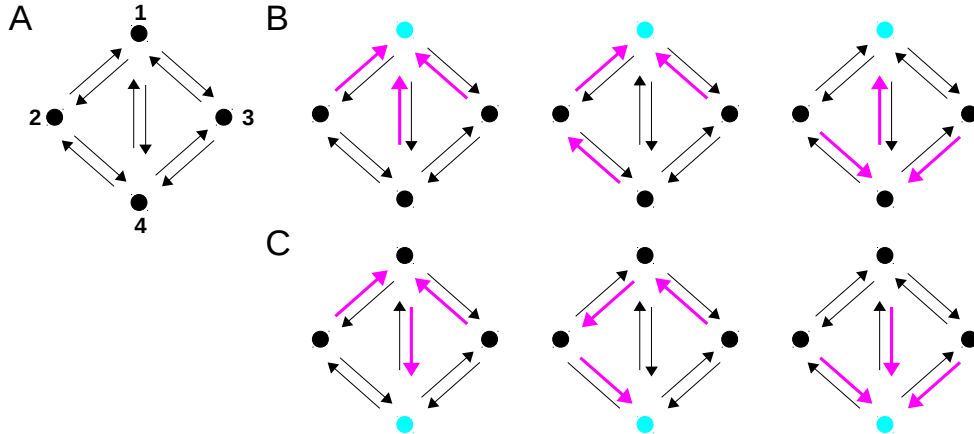


Figure 1: Graphs and spanning trees. **A** Reversible linear framework graph, with named vertices and labels omitted. **B** Three spanning trees (magenta edges) rooted at vertex 1 (cyan), chosen from 8 possibilities. **C** Corresponding spanning trees rooted at vertex 4, obtained by applying the map  $\Phi_{1,4}$ , as described in the text, to the tree vertically above in panel **B**, with the same colour code as **B**.

## RESULTS

### Steady-state probabilities in the linear framework

We briefly describe the linear framework. More details and background can be found in [14, 26, 9, 3, 37]. Let  $G$  denote a finite, directed graph with labelled edges and no self-loops (Fig.1A). We denote the vertices of  $G$  by the indices,  $1, 2, \dots, n$ , an edge from  $i$  to  $j$  by  $i \rightarrow j$  and the label on this edge by  $\ell(i \rightarrow j)$ . We think of the vertices as mesostates of the system under study, implying thereby that they are coarse-grained abstractions of the underlying physical microstates. The edges correspond to transitions between mesostates with the label being the transition rate, with dimensions of  $(\text{time})^{-1}$ . Labels may be complex expressions which describe interactions between mesostates and environmental reservoirs, such as those for molecular entities (particles) or heat. We make the customary thermodynamic assumption that exchanges between the graph and the reservoirs, for instance through binding or unbinding of a ligand, do not change the thermodynamic potentials of the reservoirs. Edge labels may then be treated as constants.

$G$  describes the infinitesimal generator of a continuous-time Markov process,  $X(t)$ , given by a conditional probability distribution on the same mesostates for times  $s > t$ ,  $\Pr(X(s) = j | X(t) = i)$ .

The edge labels are those infinitesimal transition rates,

$$\ell(i \rightarrow j) = \lim_{\Delta t \rightarrow 0} \frac{\Pr(X(t + \Delta t) = j | X(t) = i)}{\Delta t}, \quad (1)$$

which are not zero. Provided the limits in Eq.1 exist, there is an exact correspondence between Markov processes and graph representations [26]. In particular, the master equation of the Markov process, which describes the deterministic time evolution of the probabilities of mesostates, can be recovered from the graph. Let  $u_i(t)$  denote the probability of mesostate  $i$  at time  $t$ ,  $u_i(t) = \Pr(X(t) = i)$ . The master equation is the linear matrix equation

$$\frac{du(t)}{dt} = \mathcal{L}(G)u(t), \quad (2)$$

where  $\mathcal{L}(G)$  is the  $n \times n$  Laplacian matrix of  $G$  [14].

Since Eq.2 is linear, there is no difficulty in solving it in terms of eigenvalues but these are not known in terms of the edge labels, at least for  $n \geq 5$ . However, the s.s. probabilities of the mesostates, denoted  $u^*(G)$ , can be expressed in terms of the labels. If  $H$  is a subgraph of  $G$ , let  $q(H)$  denote the product of the labels on the edges of  $H$ :  $q(H) = \prod_{i \rightarrow j \in H} \ell(i \rightarrow j)$ . Let  $\Theta_i(G)$  denote the set of spanning trees of  $G$  rooted at  $i$ . A spanning tree is a subgraph which includes each vertex of  $G$  (spanning) and has no cycles if edge directions are ignored (tree); it is rooted at  $i$  if the tree has no edges outgoing from  $i$  (Fig.1B). Provided  $G$  is strongly connected, so that any two vertices,  $i$  and  $j$ , are joined by a directed path,  $i = i_1 \rightarrow i_2 \rightarrow \dots \rightarrow i_k = j$ , there exist rooted spanning trees at each vertex. Moreover, the kernel of  $\mathcal{L}(G)$  is one dimensional. A canonical basis element,  $\rho(G) \in \ker \mathcal{L}(G)$ , is given by the Matrix-Tree theorem (MTT),

$$\rho_i(G) = \sum_{T \in \Theta_i(G)} q(T). \quad (3)$$

Since  $u^*(G) \in \ker \mathcal{L}(G)$ , it follows that  $u^*(G) \propto \rho(G)$ . The proportionality constant comes from solving for total probability,  $u_1^*(G) + \dots + u_n^*(G) = 1$ , which gives,

$$u_i^*(G) = \frac{\rho_i(G)}{\rho_1(G) + \dots + \rho_n(G)}. \quad (4)$$

## Path entropies and thermodynamic equilibrium

We assume from now on that  $G$  is reversible: if  $i \rightarrow j$ , then also  $j \rightarrow i$ , and, furthermore, the reverse edge represents the reverse process to the forward edge and not simply some alternative process for moving between the mesostates. The log label ratio,  $\ln[\ell(i \rightarrow j)/\ell(j \rightarrow i)]$  is then the total entropy change in taking the transition from  $i$  to  $j$ : the entropy change in the reservoirs together with the internal entropy difference between  $j$  and  $i$ . This form of “local detailed balance” goes back to Hill and Schnakenberg and has been broadly justified within stochastic thermodynamics [31, 2]. Let  $R(i, j)$  denote the set of reversible paths,  $i = i_1 \rightleftharpoons i_2 \rightleftharpoons \dots \rightleftharpoons i_k = j$  from  $i$  to  $j$ . If  $P \in R(i, j)$  is such a path, let  $S(P)$  denote the total entropy change, as above, along the path. Evidently,

$$S(P) = \ln \left[ \left( \frac{\ell(i_1 \rightarrow i_2)}{\ell(i_2 \rightarrow i_1)} \right) \dots \left( \frac{\ell(i_{k-1} \rightarrow i_k)}{\ell(i_k \rightarrow i_{k-1})} \right) \right]. \quad (5)$$

If  $P \in R(i, j)$ , let  $P^* \in R(j, i)$  denote the reverse path, so that  $S(P^*) = -S(P)$ .

If the graph can reach thermodynamic equilibrium, an alternative basis element,  $\mu(G) \in \ker \mathcal{L}(G)$ , may be found. In this case, detailed balance holds: each pair of reversible edges,  $i \rightleftharpoons j$ , is in s.s. flux balance, so that  $u_i^*(G)\ell(i \rightarrow j) = u_j^*(G)\ell(j \rightarrow i)$ . Equivalently, given any cycle of reversible edges,  $Q \in R(i, i)$ ,  $S(Q) = 0$ . Hence, if  $P_1, P_2 \in R(i, j)$ , then  $S(P_1) = S(P_2)$ . We can then define  $\mu_i(G) = \exp(-S(P))$  for any  $P \in R(i, 1)$ . As before,  $u^*(G) \propto \mu(G)$ , which gives the following specification for equilibrium steady-state probabilities,

$$u_i^*(G) \propto \exp(-S(P)), \quad (6)$$

for any  $P \in R(i, 1)$ . A similar formula to Eq.4 holds, with  $\mu$  in place of  $\rho$ . This formula is the prescription of equilibrium statistical mechanics, with the denominator,  $\mu_1(G) + \dots + \mu_n(G)$ , being the partition function.

## Reformulating steady-state probabilities

Path entropies enable the first step in reformulating Eq.3. Following [36], let  $\Phi_{i,j} : \Theta_i(G) \rightarrow \Theta_j(G)$  be defined as follows. Choose  $T \in \Theta_i(G)$ . By construction, there is a unique path in  $T$  from  $j$  to  $i$ . Since it has no repeated vertices, this path is minimal. Reversing the edges on this minimal path

yields a spanning tree rooted at  $j$ , which is  $\Phi_{i,j}(T) \in \Theta_j(G)$  (Fig.1C).  $\Phi_{i,j}$  is a bijection—there are the same number of spanning trees at each vertex of a reversible graph—and  $\Phi_{i,j}^{-1} = \Phi_{j,i}$  [36]. Let  $M(i,j) \subseteq R(i,j)$  be the set of minimal paths from  $i$  to  $j$ . While  $R(i,j)$  is infinite,  $M(i,j)$  is finite. If we focus on the reference vertex and consider any  $T \in \Theta_1(G)$ , let  $T_i \in M(i,1)$  be the unique minimal path, as in the definition of  $\Phi_{1,i}$ . It is easy to see that [36],  $q(\Phi_{1,i}(T)) = \exp(S(T_i^*))q(T)$ . Because  $\Phi_{i,j}$  is a bijection, we can rewrite Eq.3 for any vertex  $i$  in terms of only the spanning trees rooted at 1. Recalling that  $S(T_i^*) = -S(T_i)$ , we see that (compare [23, Prop.2.1]),

$$\rho_i(G) = \sum_{T \in \Theta_1(G)} \exp(-S(T_i))q(T). \quad (7)$$

The second step in reformulating Eq.3 requires that the edge labels are expressed in Arrhenius form,  $\ell(i \rightarrow j) = \exp(\epsilon_i - W_{i \rightarrow j})$ . This form also emerges from large-deviation theory, with the temperature, which is not introduced here, playing the role of the small parameter. Here,  $\epsilon_i$  can be thought of as a vertex energy for mesostate  $i$  and  $W_{i \rightarrow j}$  as the resulting barrier energy of the edge from  $i$  to  $j$ . In general,  $W_{i \rightarrow j} \neq W_{j \rightarrow i}$ . Such a representation is always numerically possible but not unique, since units may be changed and vertex energies arbitrarily chosen: any quantity may be added to  $\epsilon_i$ , and to  $W_{i \rightarrow j}$  for all edges outgoing from  $i$ , leaving labels unchanged. Choose an Arrhenius representation and let  $T \in \Theta_1(G)$ . The energy of  $T$ ,  $E(T)$ , is defined to be,

$$E(T) = \sum_{i \rightarrow j \in T} W_{i \rightarrow j}. \quad (8)$$

We can now define the “arboreal distribution” as the Boltzman-like probability distribution on  $\Theta_1(G)$  such that  $\Pr_{\Theta_1(G)}(T) \propto \exp(-E(T))$ . Letting  $\Pi(G) = \sum_{T \in \Theta_1(G)} \exp(-E(T))$  be the normalising factor,

$$\Pr_{\Theta_1(G)}(T) = \frac{\exp(-E(T))}{\Pi(G)}. \quad (9)$$

If a different Arrhenius representation is chosen, say  $\epsilon'_i = \epsilon_i + A_i$  and  $W'_{i \rightarrow j} = W_{i \rightarrow j} + A_i$ , then tree energies are rescaled,  $E'(T) = E(T) + (A_1 + \dots + A_n)$  and the probability distribution in Eq.9 remains unchanged. Since  $q(T) = \exp(\sum_{1 \leq i \leq n} \epsilon_i) \exp(-E(T))$ , we can now rewrite  $\rho_i(G)$  in Eq.7

as,

$$\exp\left(\sum_{i=1}^n \epsilon_i\right) \Pi(G) \left( \sum_{T \in \Theta_1(G)} \exp(-S(T)) \Pr_{\Theta_1(G)}(T) \right).$$

Ignoring the initial scalar terms, this defines an alternative basis element,  $\kappa(G) \in \ker \mathcal{L}(G)$ , given by  $\kappa_i(G) = \sum_{T \in \Theta_1(G)} \exp(-S(T)) \Pr_{\Theta_1(G)}(T)$ . As before,  $u^*(G) \propto \kappa(G)$  so that we can write

$$u_i^*(G) \propto \langle \exp(-S(T_i)) \rangle, \quad (10)$$

where the brackets denote the average over the arboreal distribution on  $\Theta_1(G)$ .

Eq.10 is our reformulation of s.s. probabilities. In contrast to the MTT in Eq.3, which lacks thermodynamic meaning, Eq.10 smoothly generalises the equilibrium formula in Eq.6. At equilibrium, s.s. probabilities are given by path entropies:  $u_i^* \propto \exp(-S(P))$ . Away from equilibrium, they are given by averages over path entropies:  $u_i^* \propto \langle \exp(-S(T_i)) \rangle$ , where the average is calculated over the arboreal distribution. At equilibrium, the entropies of all paths in  $R(i, 1)$  are identical; the arboreal distribution can be factored out and Eq.10 reduces to Eq.6.

### Combinatorial scaling by energetic edges

Eq.10 has a further important advantage. Unlike rooted spanning trees, minimal path entropies do not scale with the size of the graph. Suppose that  $G$  satisfies detailed balance and let  $\ell_{eq}(i \rightarrow j)$  denote the edge labels under this condition. Suppose that edge labels are altered to break detailed balance and the new labels are given by  $\ell(i \rightarrow j) = m(i \rightarrow j) \ell_{eq}(i \rightarrow j)$ . We will say that  $i \rightarrow j$  is an *energetic edge* if  $m(i \rightarrow j) \neq 1$ . Let  $P : v = v_1 \rightleftharpoons \dots \rightleftharpoons v_k = w \in R(v, w)$  and define  $F(P)$  to be the set of energetic edges in the forward direction of  $P$ ,

$$F(P) = \{v_l \rightarrow v_{l+1} \mid m(v_l \rightarrow v_{l+1}) \neq 1\}. \quad (11)$$

The set of energetic edges in the reverse direction is then  $F(P^*)$ . It follows from Eq.5 that

$$S(P) = \ln \left[ \frac{\prod_{i \rightarrow j \in F(P)} m(i \rightarrow j)}{\prod_{i \rightarrow j \in F(P^*)} m(i \rightarrow j)} \right] + S_{eq}(P), \quad (12)$$

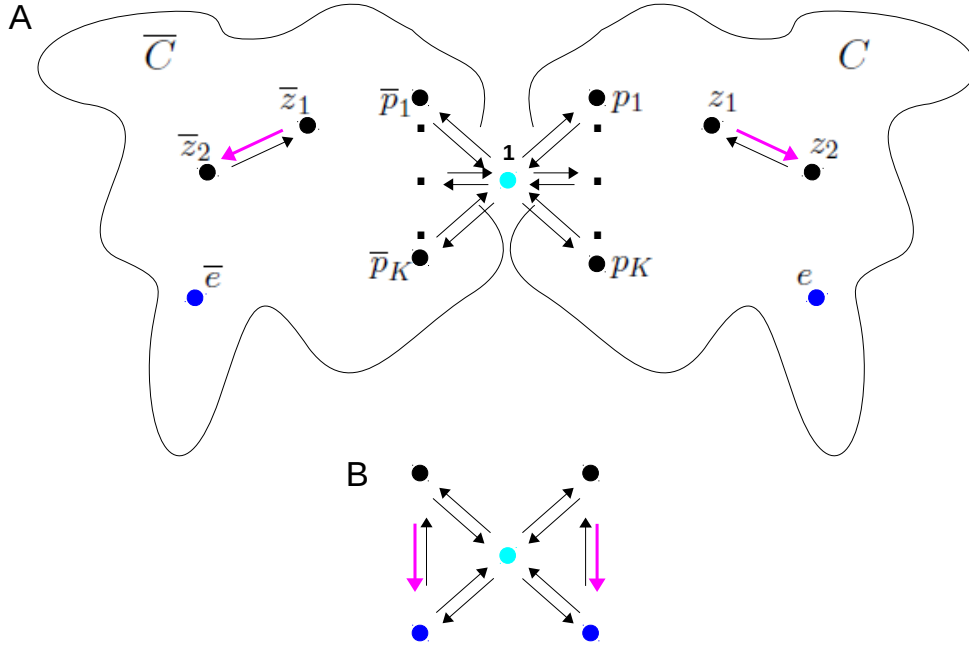


Figure 2: Hopfield discrimination. **A** Schematic butterfly graph,  $G = \bar{C} \bowtie C$ , for generalised Hopfield discrimination. The subgraphs  $C$  and  $\bar{C}$  for discriminating the correct and incorrect substrate, respectively, are structurally mirror images with a shared reference vertex (cyan).  $C$  is essentially arbitrary (cloud outline—see the text), with  $K$  proximal vertices, a single energetic edge (magenta) and an exit vertex (blue). Labels omitted for clarity. **B** The butterfly graph for Hopfield’s original analysis [35].

where  $S_{eq}(P)$  is the total entropy change along  $P$  at thermodynamic equilibrium. As noted previously,  $S_{eq}(P)$  is independent of  $P \in R(v, w)$ . Given  $P_1, P_2 \in R(v, w)$ , we will say that  $P_1$  is *energetically similar* to  $P_2$ , denoted  $P_1 \sim P_2$ , if  $F(P_1) = F(P_2)$  and  $F(P_1^*) = F(P_2^*)$ . It follows from Eq.12 that if  $P_1 \sim P_2$ , then  $S(P_1) = S(P_2)$ . Hence, the number of distinct minimal path entropies in Eq.10 is independent of the size of the graph and depends only on the number of energetic edges. This scaling still incurs a combinatorial increase, since minimal paths may have different subsets of energetic edges, but the scaling is substantially less intimidating than that arising from all rooted spanning trees (above). We examine below the implications of this scaling for a graph with a single energetic edge.

## Generalised Hopfield discrimination

Hopfield’s analysis of discrimination between a correct and incorrect substrate sought to explain the low error rates in RNA and DNA synthesis [17]. Here, we analyse a general mechanism of Hopfield discrimination using the linear framework approach of [35]. Fig.2A shows a butterfly graph,  $G = \bar{C} \bowtie C$ , consisting of two “wings”,  $\bar{C}$  and  $C$ , sharing a common reference vertex, 1, (cyan). If  $C$  and  $\bar{C}$  are strongly connected, so too is  $G$ , and [35],

$$\rho_i(G) = \begin{cases} \rho_i(\bar{C})\rho_1(C) & \text{if } i \in \bar{C} \\ \rho_1(\bar{C})\rho_i(C) & \text{if } i \in C. \end{cases} \quad (13)$$

For Hopfield discrimination,  $C$  represents the mesostates interacting with the correct substrate and  $\bar{C}$  the same for the incorrect substrate. Structurally (ie: ignoring labels),  $C$  and  $\bar{C}$  are mirror images of each other. Using overlines to map graph entities in  $C$  to their mirror images in  $\bar{C}$ ,  $i \rightarrow j$  if, and only if,  $\bar{i} \rightarrow \bar{j}$ .  $C$  is assumed to be reversible and strongly connected but otherwise arbitrary. Ligand binding to vertex 1 leads to  $K$  proximal vertices,  $p_1, \dots, p_K$  and ligand is selected to be correct at a distinguished *exit vertex*,  $e \neq 1$ . The *error ratio* is,

$$\varepsilon = \frac{u_e^*(G)}{u_e^*(G)} = \frac{\rho_{\bar{e}}(\bar{C})\rho_1(C)}{\rho_1(\bar{C})\rho_e(C)}. \quad (14)$$

where the second equality comes from Eqs.4 and 13. Assume to begin with that  $G$  is at thermodynamic equilibrium with labels  $\ell_{eq}(i \rightarrow j)$ . Following Hopfield, discrimination only takes place through unbinding from proximal vertices. Accordingly,  $\ell_{eq}(i \rightarrow j) = \ell_{eq}(\bar{i} \rightarrow \bar{j})$  as long as  $j \neq 1$  and  $\ell_{eq}(\bar{p}_u \rightarrow 1) = \alpha \ell_{eq}(p_u \rightarrow 1)$ , where  $\alpha > 1$ , so that the incorrect substrate has a higher off rate. Using Eq.6, it follows that the equilibrium error ratio is  $\varepsilon_{eq} = \alpha^{-1}$ . Accordingly,  $\varepsilon_{eq} < 1$ .

Hopfield’s insight was that  $\varepsilon_{eq}$  is independent of the number of discriminations,  $K$ , and the only way to exceed this “Hopfield barrier” [9] is to expend energy. He analysed the graph in Fig.2B, for which  $K = 2$  and  $C$  has only three vertices, with energy expenditure on the magenta edge, and identified a parametric region for kinetic proofreading in which  $(\varepsilon_{eq})^2 < \varepsilon < \varepsilon_{eq}$  [17, 35]. The question we ask here is how good  $\varepsilon$  can be when  $K > 2$  and  $C$  is a general graph (Fig.2A) in which energy is expended at only a single energetic edge (magenta) with  $\ell(z_1 \rightarrow z_2) = m \ell_{eq}(z_1 \rightarrow z_2)$ .

To answer this, we calculate how  $\varepsilon$  depends on  $m$  and  $\alpha$  by using the reformulation above, with Eq.7 being more convenient for this purpose than Eq.10, and by partitioning trees according to proximal edges (ie: edges  $j \rightarrow 1$ , where  $j$  is a proximal vertex). We give a sketch here, with details in the Supplementary Information.

Given a polynomial  $\mathcal{P}$  in the edge labels, we say that it is  $m$ -free, respectively  $\alpha$ -free, if  $m$ , respectively  $\alpha$ , does not divide any monomial in  $\mathcal{P}$ . Let  $\Theta = \Theta_1(G)$ . Eq.7 leads us to partition  $\Theta$  according to the combinatorics of the energetic edge on minimal paths in  $M(e, 1)$ ,

$$\begin{aligned}\Theta_0 &= \{T \in \Theta \mid z_1 \rightarrow z_2, z_2 \rightarrow z_1 \notin T_e\} \\ \Theta_+ &= \{T \in \Theta \mid z_2 \rightarrow z_1 \in T_e\} \\ \Theta_- &= \{T \in \Theta \mid z_1 \rightarrow z_2 \in T_e\}.\end{aligned}\tag{15}$$

Let  $P_0, P_+, P_- \in M(e, 1)$  be any choices of minimal paths arising as  $T_e$  for  $T \in \Theta_0, \Theta_+, \Theta_-$ , respectively. By construction, different choices are energetically similar, so that  $S(P_0), S(P_+), S(P_-)$  are well defined for any choices of minimal paths. Furthermore, by Eq.12,  $S(P_+) = S(P_0) - \ln(m)$ ,  $S(P_-) = S(P_0) + \ln(m)$ . Let us extend  $q$  to subsets  $X \subseteq \Theta$  by defining  $q(X) = \sum_{T \in X} q(T)$  and note that  $q_{eq}$  corresponds to  $m = 1$ . We see from Eq.15 that  $q(\Theta_+)$  is  $m$ -free and that  $q(\Theta_-) = m q_{eq}(\Theta_-)$ . Hence we can rewrite Eq.7 as,

$$\rho_e(C) = \exp(-S(P_0)) (q(\Theta_0) + m q(\Theta_+) + q_{eq}(\Theta_-)) ,\tag{16}$$

where  $q(\Theta_0)$  and  $q_{eq}(\Theta_-)$  are  $m$ -free but  $q(\Theta_0)$  may not be.

We now introduce the partitioning scheme. Given  $X \subseteq \Theta$ , let  $X^{(j,u)} \subseteq X$ , for  $1 \leq j \leq K$  and  $0 \leq u \leq 1$ , consist of those trees in  $X$  with exactly  $j$  proximal edges to 1 and exactly  $u$  energetic edges. The  $X^{(j,u)}$  form a partition of  $X$  into mutually disjoint subsets, so that  $q(X) = \sum_{j,u} q(X^{(j,u)})$ . By construction,  $q(X^{(j,0)})$  is  $m$ -free and  $q(X^{(j,1)}) = m q_{eq}(X^{(j,1)})$ , where  $q_{eq}(X^{(j,1)})$  is  $m$ -free. Most importantly, again by construction,

$$q(\overline{X}^{(j,u)}) = \alpha^j q(X^{(j,u)}),\tag{17}$$

where, evidently,  $q(X^{(j,u)})$  is  $\alpha$ -free.

Eqs.16 and 17 make it straightforward to calculate the error ratio from Eq.14,

$$\varepsilon = \varepsilon_{eq} \left( \frac{(\overline{P}m + \overline{Q})(Rm + S)}{(\overline{R}m + \overline{S})(Pm + Q)} \right), \quad (18)$$

where the eight quantities in Eq.18, which are all  $m$ -free, are expressed in terms of the constructions introduced above. It is striking that Eq.18 has the same algebraic form for the general graph in Fig.1A as for Hopfield's simple graph in Fig.1B (compare [35, Eq.4]), albeit with vastly more complicated coefficients. The overlined coefficients in Eq.18 are each of degree  $K$  in  $\alpha = \varepsilon_{eq}^{-1}$ . It is now straightforward to show that,

$$(\varepsilon_{eq})^K < \varepsilon < (\varepsilon_{eq})^{2-K}. \quad (19)$$

The left-hand inequality in Eq.19 generalises Hopfield's finding for Fig.1B with  $K = 2$ .

## DISCUSSION

The Matrix-Tree theorem (MTT) gives an exact solution, in terms of the edge labels or transition rates, for the s.s. probabilities of a Markov process (Eq.3). The MTT's elegant mathematical statement belies its intractability. Away from thermodynamic equilibrium, the s.s. probability of a vertex,  $i$ , is globally dependent on all edge labels in the graph, in stark contrast to equilibrium, in which only the edge labels on a minimal path in  $M(1, i)$  are relevant (Eq.6). At equilibrium, s.s. probabilities are path independent; away from equilibrium they are not merely path dependent but every path in  $M(1, i)$  is needed and the MTT does the bookkeeping for this calculation by way of spanning trees (Eq.3). This requires enumerating all spanning trees rooted at  $i$ , leading to a combinatorial explosion that leaves even simple graphs beyond the reach of calculation. Studies have had to rely, in effect, on astute approximations to a few dominant trees. While this has provided important insights it also suggests that those behaviours which depend on small contributions from many trees may have been overlooked. This could be a particularly serious omission in biology, where functionality can arise from many small contributions [5].

We have overcome the intractability of s.s. probabilities in two ways. First, by recasting the MTT in thermodynamic terms as a generalisation of the equilibrium case: in place of minimal path

entropies at equilibrium (Eq.6), averages of these quantities must be taken away from equilibrium (Eq.10). Here, the average is calculated over the Boltzman-like probability distribution on spanning trees which we call the arboreal distribution (Eq.9). Second, energetically similar minimal paths have identical entropies so that the number of distinct minimal path entropies scales with the number of energetic edges and not the size of the graph. It is this scaling which has enabled exact calculation of the error ratio for generalised Hopfield discrimination (Eq.18), for an arbitrary graph with only a single energetic edge (Fig.2A). Such a calculation would have remained intractable with the un-reformulated MTT [27].

The reformulation in Eq.10 is appealing, in part, because of its formal resemblance to other path ensemble formulations in physics. In quantum mechanics, the probability amplitude for a particle going from  $A$  to  $B$  is the integral over all paths from  $A$  to  $B$  of the action along the paths [11]. In statistical mechanics, equilibrium information can be recovered from driven non-equilibrium paths by averaging the exponential of the work performed along the paths [18] and many exact non-equilibrium fluctuation theorems can be obtained in this way [6]. Interestingly, in the present paper, it is non-equilibrium information which is recovered from a Boltzman-like distribution. Whether some more fundamental setting underlies these different path ensemble formulations is beyond the scope of this paper but we note how essential the graph-theoretic framework is to clarifying the ensemble. We cannot speak of “paths” without the graph and it is the graph which yields the spanning trees on which the arboreal distribution is defined. The reformulation reinforces the central role of the graph in the non-equilibrium behaviour of Markov processes, testifying again to the pioneering insights of Hill and Schnakenberg.

The graph also clarifies Hopfield’s analysis of kinetic proofreading [17]. At equilibrium, path independence of s.s. probabilities (Eq.6) implies that the system cannot tell how many discriminations have been made, so that  $\varepsilon_{eq}$  is independent of their number. Away from equilibrium, path dependency allows in principle for a profoundly different behaviour, in which energy dissipation, even locally at a single edge, can enable multiple discriminations to collectively reduce the error (Eq.19). It remains an open problem to determine under what conditions optimal discrimination is possible, for which  $(\varepsilon_{eq})^K < \varepsilon < (\varepsilon_{eq})^{K-1}$ . The approach developed here suggests potential solutions, which we hope to discuss in subsequent work.

The arboreal distribution is central to our reformulation (Eq.10) but remains curiously elusive.

At equilibrium, it factors out of the expression for s.s. probabilities (Eq.6). Away from equilibrium, it concentrates on the much reduced distribution determined by the energetic edges, yielding only three terms for one energetic edge (Eq.16). A richer characterisation of the arboreal distribution remains another important problem for future work.

A final thought comes from Eq.19, whose bounds suggest that the non-equilibrium error ratio can exceed the equilibrium value  $\varepsilon_{eq}$ . This does indeed happen: expending energy can yield worse outcomes than at equilibrium [27]. We see that being “away from equilibrium” is not a simple condition but, rather, a door into a nuanced and complex landscape, in which how and where energy is expended can substantially influence functional outcomes. The ideas introduced here suggest that we can begin to “follow the energy” through this non-equilibrium landscape to uncover the logic of biological information processing.

## SUPPLEMENTARY INFORMATION

We provide further details here of the analysis of generalised Hopfield discrimination, following on from the main text and the notation introduced there. The goal is to calculate the error ratio,  $\varepsilon$ , and prove Eqs.18 and 19 of the main text.

### Partitioning scheme

Let us recall the partitioning scheme in which a subset of spanning trees rooted at the reference vertex,  $X \subseteq \Theta$ , is divided into parts,  $X^{(j,u)}$ , for  $1 \leq j \leq K$  and  $0 \leq u \leq 1$ .  $X^{(j,u)}$  consists of those trees in  $X$  with exactly  $j$  proximal edges to 1 and exactly  $u$  energetic edges. In other words,  $T \in X^{(j,u)}$  if, and only if, there are distinct proximal vertices,  $p_{i_1}, \dots, p_{i_j}$  in  $C$ , which may depend on  $T$ , such that  $p_{i_1} \rightarrow 1, \dots, p_{i_j} \rightarrow 1 \in T$  but no other proximal vertices have this property; and, if  $u = 0$ ,  $z_1 \rightarrow z_2 \notin T$ , while if  $u = 1$ ,  $z_1 \rightarrow z_2 \in T$ . Note that any tree in  $\Theta$  must have between 1 and  $K$  proximal edges to 1 and no more than 1 energetic edge (Fig.2A in the main text). It follows that the  $X^{(j,u)}$  form a partition of  $X$  into disjoint subsets,

$$X = (X^{(1,0)} \amalg X^{(1,1)}) \amalg \dots \amalg (X^{(K,0)} \amalg X^{(K,1)}). \quad (20)$$

Hence, we can decompose  $q(X)$  as follows,

$$\begin{aligned} q(X) &= \left( q(X^{(1,0)}) + \dots + q(X^{(K,0)}) \right) \\ &\quad + m \left( q_{eq}(X^{(1,1)}) + \dots + q_{eq}(X^{(K,1)}) \right) \end{aligned} \quad (21)$$

where the terms  $q(X^{(j,0)})$  and  $q_{eq}(X^{(j,1)})$  are all  $m$ -free. The value of this decomposition becomes clear by applying Eq.17 of the main text to see that,

$$\begin{aligned} q(\bar{X}) &= \left( \alpha q(X^{(1,0)}) + \dots + \alpha^K q(X^{(K,0)}) \right) \\ &\quad + m \left( \alpha q_{eq}(X^{(1,1)}) + \dots + \alpha^K q_{eq}(X^{(K,1)}) \right), \end{aligned} \quad (22)$$

where the expressions  $q(X^{(j,0)})$  and  $q_{eq}(X^{(j,1)})$  are both  $m$ -free, as above, and, by construction,  $\alpha$ -free.

### Calculation of $\rho_1(C)$ and $\rho_1(\bar{C})$

Let us abbreviate  $\sum_{1 \leq j \leq K}$  by  $\sum_j$ . Since  $\rho_1(C) = q(\Theta)$ , it follows from Eq.21 that,

$$\rho_1(C) = \left( \sum_j q(\Theta^{(j,0)}) \right) + m \left( \sum_j q_{eq}(\Theta^{(j,1)}) \right). \quad (23)$$

Similarly, applying Eq.22 to  $\rho_1(\bar{C}) = q(\bar{\Theta})$ , we see that,

$$\rho_1(\bar{C}) = \left( \sum_j \alpha^j q(\Theta^{(j,0)}) \right) + m \left( \sum_j \alpha^j q_{eq}(\Theta^{(j,1)}) \right). \quad (24)$$

### Calculation of $\rho_e(C)$ and $\rho_{\bar{e}}(\bar{C})$

We begin with Eq.16 of the main text which represented  $\rho_e(C)$  in terms of a partition into disjoint subsets of  $\Theta$ ,

$$\Theta = \Theta_0 \amalg \Theta_+ \amalg \Theta_- \quad (25)$$

It is clear from Eq.16 of the main text that, for all  $1 \leq j \leq K$ ,

$$\Theta_+^{(j,1)} = \emptyset \text{ and } \Theta_-^{(j,0)} = \emptyset. \quad (26)$$

If we now apply the decomposition in Eq.21 to each of the three subsets of Eq.25, and collect together the  $m$ -free terms in Eq.16 of the main text, we find that,

$$\begin{aligned} \rho_e(C) = & \exp(-S(P_0)) \times \\ & \left[ \sum_j \left( q(\Theta_0^{(j,0)}) + q_{eq}(\Theta_-^{(j,1)}) \right) \right. \\ & \left. + m \left( \sum_j \left( q_{eq}(\Theta_0^{(j,1)}) + q(\Theta_+^{(j,0)}) \right) \right) \right]. \end{aligned} \quad (27)$$

Similarly, using the decomposition in Eq.22, we find that,

$$\begin{aligned} \rho_{\bar{e}}(\bar{C}) = & \alpha^{-1} \exp(-S(P_0)) \times \\ & \left[ \sum_j \alpha^j \left( q(\Theta_0^{(j,0)}) + q_{eq}(\Theta_-^{(j,1)}) \right) \right. \\ & \left. + m \left( \sum_j \alpha^j \left( q_{eq}(\Theta_0^{(j,1)}) + q(\Theta_+^{(j,0)}) \right) \right) \right], \end{aligned} \quad (28)$$

where we have used the fact that  $S(\overline{P}_0) = \alpha^{-1}S(P_0)$ .

### Proof of Eq.18 of the main text

We have now calculated each of the four terms appearing in Eq.18 of the main text. Using overlines again to indicate coefficients from the mirror image subgraph  $\overline{C}$  and recalling from the main text that  $\alpha = (\varepsilon_{eq})^{-1}$ , we find that,

$$\varepsilon = \varepsilon_{eq} \left( \frac{(\overline{P}m + \overline{Q})(Rm + S)}{(\overline{R}m + \overline{S})(Pm + Q)} \right). \quad (29)$$

The eight coefficients in Eq.29 are given by

$$\begin{aligned} P &= \sum_j q_{eq}(\Theta_0^{(j,1)}) + q(\Theta_+^{(j,0)}) \\ Q &= \sum_j q(\Theta_0^{(j,0)}) + q_{eq}(\Theta_-^{(j,1)}) \\ R &= \sum_j q_{eq}(\Theta^{(j,1)}) \\ S &= \sum_j q(\Theta^{(j,0)}) \\ \overline{P} &= \sum_j \alpha^j (q_{eq}(\Theta_0^{(j,1)}) + q(\Theta_+^{(j,0)})) \\ \overline{Q} &= \sum_j \alpha^j (q(\Theta_0^{(j,0)}) + q_{eq}(\Theta_-^{(j,1)})) \\ \overline{R} &= \sum_j \alpha^j q_{eq}(\Theta^{(j,1)}) \\ \overline{S} &= \sum_j \alpha^j q(\Theta^{(j,0)}). \end{aligned} \quad (30)$$

The various expressions of the form  $q(-)$  or  $q_{eq}(-)$  in Eq.30 are all both  $\alpha$ -free and  $m$ -free. Eq.29 establishes Eq.18 of the main text.

### Proof of Eq.19 of the main text

Using the fact that  $\alpha > 1$ , which encodes the distinction between the correct and incorrect substrate, we see by inspection of Eq.30, that

$$\begin{aligned} \alpha(P + Q) &< \overline{P} + \overline{Q} < \alpha^K(P + Q) \\ \alpha(R + S) &< \overline{R} + \overline{S} < \alpha^K(R + S). \end{aligned}$$

It follows that

$$\alpha < \frac{\overline{P} + \overline{Q}}{P + Q} < \alpha^K \quad (31)$$

and also that

$$\alpha^{-K} < \frac{R + S}{\overline{R} + \overline{S}} < \alpha^{-1} \quad (32)$$

Combining Eqs.31 and 32 and using Eq.29 and the fact that  $\alpha = (\varepsilon_{eq})^{-1}$ , we see that,

$$(\varepsilon_{eq})^K < \varepsilon < (\varepsilon_{eq})^{2-K}, \quad (33)$$

which proves Eq.19 of the main text.

## ACKNOWLEDGEMENTS

U.C. was supported by the Giovanni Armenise Harvard Foundation and J.G. was supported by US National Science Foundation award #1462629.

## References

- [1] D. Andrieux and P. Gaspard. Fluctuation theorem for currents and Schnakenberg network theory. *J. Stat. Phys.*, 127:107–31, 2007.
- [2] M. Bauer and F. Cornu. Local detailed balance: a microscopic derivation. *J. Phys. A: Math. Theor.*, 48:015008, 2015.
- [3] J. W. Biddle, M. Nguyen, and J. Gunawardena. Negative reciprocity, not ordered assembly, underlies the interaction of Sox2 and Oct4 on DNA. *eLife*, 8:e410172018, 2019.
- [4] M. Cameron and E. Vanden-Eijnden. Flows in complex networks: theory, algorithms, and application to Lennard-Jones cluster rearrangement. *J. Stat. Phys.*, 156:427–54, 2014.
- [5] J. Crocker, N. Abe, L. Rinaldi, A. P. McGregor, N. Frankel, S. Wang, A. Alsawadi, P. Valenti, S. Plaza, F. Payre, R. S. Mann, and D. L. Stern. Low affinity binding site clusters confer Hox specificity and regulatory robustness. *Cell*, 160:191–203, 2015.
- [6] G. E. Crooks. Path-ensemble averages in systems driven far from equilibrium. *Phys. Rev. E*, 61:2361–6, 2000.
- [7] Gavin E Crooks. Entropy production fluctuation theorem and the nonequilibrium work relation for free energy differences. *Physical Review E*, 60(3):2721, 1999.
- [8] T. Dasgupta, D. H. Croll, J. A. Owen, M. G. Vander Heiden, J. W. Locasale, U. Alon, L. C. Cantley, and J. Gunawardena. A fundamental trade off in covalent switching and its circumvention by enzyme bifunctionality in glucose homeostasis. *J. Biol. Chem.*, 289:13010–25, 2014.
- [9] J. Estrada, F. Wong, A. DePace, and J. Gunawardena. Information integration and energy expenditure in gene regulation. *Cell*, 166:234–44, 2016.
- [10] Denis J Evans, Ezechieel GD Cohen, and Gary P Morriss. Probability of second law violations in shearing steady states. *Physical Review Letters*, 71(15):2401, 1993.
- [11] R. P. Feynman. Space-time approach to non-relativistic quantum mechanics. *Rev. Mod. Phys.*, 20:367, 1948.

- [12] M. I. Freidlin and A. D. Wentzell. *Random perturbations of dynamical systems*. Springer, Heidelberg, Germany, 3 edition, 2012.
- [13] Giovanni Gallavotti and Ezechiel Godert David Cohen. Dynamical ensembles in nonequilibrium statistical mechanics. *Physical Review Letters*, 74(14):2694, 1995.
- [14] J. Gunawardena. A linear framework for time-scale separation in nonlinear biochemical systems. *PLoS ONE*, 7:e36321, 2012.
- [15] T. L. Hill. Studies in irreversible thermodynamics IV. Diagrammatic representation of steady state fluxes for unimolecular systems. *J. Theoret. Biol.*, 10:442–59, 1966.
- [16] T. L. Hill. *Free Energy Transduction and Biochemical Cycle Kinetics*. Dover Publications, New York, USA, 2004.
- [17] J. J. Hopfield. Kinetic proofreading: a new mechanism for reducing errors in biosynthetic processes requiring high specificity. *Proc. Natl. Acad. Sci. USA*, 71:4135–39, 1974.
- [18] C. Jarzynski. Equilibrium free-energy differences from non-equilibrium measurements: a master equation approach. *Phys. Rev. E*, 56:5018–35, 1997.
- [19] Christopher Jarzynski. Nonequilibrium equality for free energy differences. *Physical Review Letters*, 78(14):2690, 1997.
- [20] G. Kirchhoff. Ueber der Auflösung der Gleichungen, auf welche man bei Untersuchung der linearen Vertheilung galvanischer Ströme geführt wird. *Annalen der Physik und Chemi*, 72:497–508, 1847.
- [21] Jorge Kurchan. Fluctuation theorem for stochastic dynamics. *Journal of Physics A: Mathematical and General*, 31(16):3719, 1998.
- [22] Joel L Lebowitz and Herbert Spohn. A Gallavotti–Cohen-type symmetry in the large deviation functional for stochastic dynamics. *Journal of Statistical Physics*, 95(1-2):333–365, 1999.
- [23] C. Maes and K. Netočný. Heat bounds and the Blowtorch Theorem. *Ann. Henri Poincaré*, 14:1193–202, 2013.

- [24] Christian Maes. The fluctuation theorem as a Gibbs property. *Journal of Statistical Physics*, 95(1-2):367–392, 1999.
- [25] I. Mirzaev and D. M. Bortz. Laplacian dynamics with synthesis and degradation. *Bull. Math. Biol.*, 77:1013–45, 2015.
- [26] I. Mirzaev and J. Gunawardena. Laplacian dynamics on general graphs. *Bull. Math. Biol.*, 75:2118–49, 2013.
- [27] A. Murugan, D. A. Huse, and S. Leibler. Discriminatory proofreading regimes in nonequilibrium systems. *Phys. Rev. X*, 4:021016, 2014.
- [28] K.-M. Nam, B. M. Gyori, S. V. Amethyst, D. J. Bates, and J. Gunawardena. Robustness and parameter geography in post-translational modification systems. *PLoS Comp. Biol.*, 16:e1007573, 2020.
- [29] J. Park, J. Estrada, G. Johnson, C. Ricci-Tam, M. Bragdon, Y. Shulgina, A. Cha, J. Gunawardena, and A. H. DePace. Dissecting the sharp response of a canonical developmental enhancer reveals multiple sources of cooperativity. *eLife*, 8:e41266, 2019.
- [30] J. Schnakenberg. Network theory of microscopic and macroscopic behaviour of master equation systems. *Rev. Mod. Phys.*, 48:571–86, 1976.
- [31] U. Seifert. Stochastic thermodynamics: principles and perspectives. *Eur. Phys. J. B*, 64:423–31, 2008.
- [32] W. T. Tutte. The dissection of equilateral triangles into equilateral triangles. *Proc. Camb. Phil. Soc.*, 44:463–82, 1948.
- [33] A. D. Ventsel’ and M. I. Freidlin. On small random dynamical perturbations of dynamical systems. *Russ. Math. Surv.*, 25:1–54, 1970.
- [34] D. J. Wales. Energy landscapes: calculating pathways and rates. *Int. Rev. Phys. Chem.*, 25:237–82, 2006.
- [35] F. Wong, A. Amir, and J. Gunawardena. Energy-speed-accuracy relation in complex networks for biological discrimination. *Phys. Rev. E.*, 98:012420, 2018.

- [36] F. Wong, A. Dutta, D. Chowdhury, and J. Gunawardena. Structural conditions on complex networks for the Michaelis-Menten input-output response. *Proc. Natl. Acad. Sci. USA*, 115:9738–43, 2018.
- [37] F. Wong and J. Gunawardena. Gene regulation in and out of equilibrium. *Annu. Rev. Biophys.*, 49:199–226, 2020.
- [38] P. Yordanov and J. Stelling. Steady-state differential dose response in biological systems. *Biophys. J.*, 114:723–36, 2018.
- [39] P. Yordanov and J. Stelling. Efficient manipulation and generation of Kirchhoff polynomials for the analysis of non-equilibrium biochemical reaction networks. *J. Roy. Soc. Interface*, 17:20190828, 2020.